

Using GNSS reflections for Ionospheric Studies

G. Ruffini¹, M. Caparrini¹, F. Soulat¹, Manuel Martin-Neira², P. Silvestrin², K. Sharman¹

¹STARLAB Barcelona SL

Phone: +34 93 2540 369, Email: {giulio,marco,paco,ken}@starlab-bcn.com

² ESA-ESTEC

Phone: +31 71 565 6565, Email: {Manuel.Martin-Neira,Pierluigi.Silvestrin}@esa.int

1 Abstract

We discuss the usefulness of GNSS-R ionospheric electron content measurements in the context of a spaceborne LEO mission. GNSS-R measurements can complement occultation measurements for applications such as ionospheric electron content tomography or direct ingestion into models, since they will provide, a) many measurements over the oceans of a b) vertical nature. We show that GNSS-R ionospheric electron content code (dual frequency) ranging measurements from missions with antenna gains bigger than 15 dB can already provide useful information. In addition, simulations show that ionospheric combination L_I phase measurements are not much affected by the scattering process and therefore that ionospheric phase can conceivably be tracked.

2 Introduction

It is well-known that the atmosphere affects the propagation of radio signals. Both the neutral troposphere and the ionosphere impact ranging measurements from radar systems. In fact, it has been an important goal for the GPS/GNSS research community to test the limits of the geophysical measurement techniques derived from this technology. Both the troposphere and the ionosphere have been an object of intense research exploiting the fact that GPS (L-band) signals are susceptible to the atmospheric gas and plasma distribution. This, together with the high precision of the GPS system, has opened a wide door to study atmospheric phenomena.

The use of GPS signals for the retrieval of electron content profiles using occultations, subject of several ESA studies [14], is already a fact. After the first success of GPS/MET and SAC-C, since February 2001 also the hundreds occultations per-day provided by CHAMP are available. The electron content vertical profiles obtained by these instruments usually assume a spherical symmetry of the ionosphere properties. Using these data in

synergy with measurements of *intrinsically* vertical nature such as those from ground GPS, a much better 4D image of the ionosphere electronic content can be generated, with applications to, e.g. radar altimeters. Tomographic techniques are potentially not as biased as is usual in TEC vertically mapping, which require assumptions on vertical distribution.

In the present paper we investigate the possible use of spaceborne GNSS Reflections (GNSS-R) to sound the ionosphere (LEO scenario, Figure 6), a possibility already discussed in [1]. This possibility would provide a higher number of **vertical, or at least oblique, bi-TEC measurements over the oceans, an important missing data element in ionospheric observation systems.**

3 GNSS-R and PARIS

GNSS-R is an offspring of the **PARIS** concept. PARIS¹ is a highly innovative Earth Observation technique which can provide new products, excellent coverage and resolution at low cost. See [7] for a review.

PARIS, an idea from the pioneering work of Martín-Neira [3], involves using reflected signals from sources of opportunity to infer properties of the ocean surface. The “sources of opportunity” in this paper are radio wave transmitters from Global Navigation Satellite Systems (GNSS), but other sources can be considered. GNSS-R is a Global Navigation Satellite System (GNSS) implementation of PARIS, carrying the possibility of multi-frequency phase ranging measurements. We note that Global Navigation Satellite Systems are ideally suited to play an important role within the Global Observation System, given their long operational life and their essentially self-calibrating nature. Two GNSS constellations are presently operational, the Global Positioning System (GPS), owned by the United States, and the Rus-

¹Passive Reflectometry and Interferometry System [3]

sian GLObal NAVigation Satellite System (GLONASS). In the next few years, the European Satellite Navigation System (GALILEO) is planned to be deployed, with the launch of the first block of satellites scheduled for 2003 and operation in 2008. When GALILEO becomes operational in 2008 more than 50 GNSS satellites will be emitting L-band spread spectrum signals with a well characterised structure, and they will remain in operation for at least a few decades. These signals can be used within the GOS, as we will now discuss.

One of PARIS' main merits in a LEO constellation incarnation stem from its inexpensive global coverage and resolution potential: PARIS is a bistatic radar system in which only the receivers need to be deployed—the emitters are already there. Furthermore, GPS is undergoing some changes (such as the addition of civilian frequencies and increased power), and Galileo will offer a variety of signals, adding even more to the possibilities.

What are the data products that can be extracted from GNSS scattered signals, and who will benefit from them? Ocean surface rugosity alters the “echoes” signature of the signals, and ocean surface rugosity depends partly on surface wind. Numerical Weather Prediction models can benefit profoundly from the availability of surface wind data on a global scale and with the potential spatial and temporal resolution provided by a space-based PARIS system. But a PARIS system can also be used in commercial aircraft, and thus provide local measurements that can be very useful to fast boat traffic at little cost, as well as provide altitude information for the aircraft.

Other data products include atmospheric measurements. As the GNSS signal crosses the atmosphere it experiences delays that depend on the ionospheric electron content and the tropospheric index of refraction. From orbit, a comparison of the relative delay between the direct and reflected signals can yield information on ionospheric electron content, tropospheric temperature, pressure and water vapour content. Although this aspect of the technique is not yet as well developed, it deserves further research because of its significant potential impact. In this paper we discuss the possibility of extracting biTEC measurements from GPS reflected signals we can see that they would add an important source of GPS data to the others available (such as ground or LEO GPS direct data). Indeed, some work in this area has already been carried out (see [1]).

Let us itemise the different data products from PARIS systems:

- Altimetry, surface topography (H).
- Directional Mean Square Slope (DMSS).
- Surface wind velocity (W).
- Phase Bandwidth/Doppler spread (B).

- Ionospheric double-path slant delay data (biTEC).
- Tropospheric double-path slant delay data (bi-TROP).
- Navigation data (N).

An important potential application is therefore Space Weather.

4 GPS signals and the ionosphere

The ionosphere adds a delay of a few meters to the GNSS signal (L band). The exact amount depends on which of the two GPS available frequencies is considered ($f_1 = 1.57542$ GHz and $f_2 = 1.22760$ GHz). GNSS-R code bistatic ranging data has an intrinsic noise of less than 0.5 meter after 1 second of integration, with the assumption of a reasonably large antenna (25 dB). Thus, this data holds great potential value to ionospheric science, even if only code ranging data is available and the phase cannot be tracked. Ionospheric tomography will benefit greatly from GNSS-R data for an additional reason: as mentioned above, it complements the geometry of occultation data (with very horizontal ray paths) very nicely. GPS and Galileo are multi-frequency systems since the ionospheric contribution to the delay can be removed by making use of its dispersive nature. In fact the linear combination of delays $D_C = (f_1^2 D_{L_1} - f_2^2 D_{L_2}) / (f_1^2 - f_2^2)$ does not depend on ionosphere. This combination is called the *ionospheric-free combination* and is not to be confused with the *ionospheric combination* L_I discussed below.

The problems of gathering data from reflections and from occultations are thus fairly similar. It is also worth mentioning here that even if only one frequency is available, comparison of phase and group ionospheric delays (of equal but opposite sign) can yield ionospheric electron estimates. Thus, under the assumption of phase tracking, ionospheric delay measurements would also be available.

We briefly review now the main concepts of GNSS ionospheric delay measurements. Consider a signal travelling at time t between a given satellite and receiver, and let $I = \int_{ray} dl \rho(\vec{x})$ be the integrated electron density along the ray traversed by the signal (in electrons per square meter). Then, the delay L_I is modelled by

$$D_{L_i}(t) = D_{s.l.}(t) - I(t) \alpha / f_i^2 + T + \tilde{c}_{sat}^i + \tilde{c}_{rec}^i + \tilde{c}_{align}^i + \text{noise} + (D^i(t) - D_{s.l.}(t)), \quad (1)$$

where $\alpha = 40.30 \text{ m}^3/\text{s}^2$, D^i is the length of the real ray, $D_{s.l.}$ is the length of the ray if it travelled in a straight line (in the vacuum), T models other frequency independent terms, and \tilde{c}_{sat}^i and \tilde{c}_{rec}^i are the instrumental biases

(which are assumed to remain constant). The term \tilde{c}_{align}^i represents the bias introduced in the alignment of the phases with pseudo-ranges. In the alignment process, the essential ambiguity of the first phase measurement in an arc is fixed by comparing the phases of one arc with the unambiguous, albeit less accurate, code pseudo-ranges. Because of the noise present in code pseudo-ranges, the alignment procedure introduces a noise bias in the phases of each arc. This noise is smaller for longer arcs. While this term is normally omitted in the case of ground networks analysis, we keep it here due to the shortness of the ray arcs involved in occultations and presumably also in GNSS-R reflections. The last term in equation (1) is the difference between the length of the real ray and the length of the ray if it propagated in the vacuum. Thus, GNSS ionospheric observables consist essentially of the delays experienced by the dual frequency signals emitted from the GNSS sources (25 GPS satellites at present) and received at the GNSS receiver. Moreover, the paths taken by the signals are essentially the same for either of the frequencies used by the GPS network. Hence, we can model the difference between the delays by

$$\begin{aligned} D_{L_I} &= D_{L_1} - D_{L_2} \\ &\approx -\alpha \left(\frac{1}{f_1^2} - \frac{1}{f_2^2} \right) \\ &\quad \int_{s.l.} dl \rho(\vec{x}) + \tilde{c}_{sat}^I + \tilde{c}_{rec}^I + \tilde{c}_{align}^I + \text{noise} \end{aligned} \quad (2)$$

(see [12] for more details), where ρ is the ionospheric electron density and the new delay constants are given by the difference between the corresponding constants at each frequency. In the ionospheric inversion problem, this is the “tomographic equation”: if enough rays are given, the corresponding set of equations can be solved to obtain estimates of ρ .

The number of equations can be very roughly estimated by

$$\# \text{ eqns} = \frac{\text{observing period}}{\text{resolution}} \cdot (\# \text{ emitters}) \cdot (\# \text{ receivers}), \quad (3)$$

where the term “resolution” refers to the amount of time needed to extract an observation with a given precision. In the case of ground networks, given that four satellites can be seen at each of more than 200 (land based) sites during an observing period of 30 seconds, we will have approximately 1000 observations from rays crossing the ionosphere. In the case of the GPS/MET orbiting receiver we have a resolution of 0.02 seconds, and during an observation period of 30 seconds we will get about 1500 observations per emitter. From GNSS-R we expect a useful observation every second over the oceans, from each of the available sources (up to 10 with joint GPS/GALILEO

constellations). Note that although the number of equations is different for these cases, their value is not, for geometrical and coverage reasons.

Despite the complementarity in the spatial distribution of the rays, depending on the spatio-temporal resolution desired we may expect singularities in the inversion process. Therefore, to specify a unique solution to the problem, additional information must be provided in the form of constraints or models (see, e.g., [8]). For example, in the ground data case it is certainly possible to add some linear constraints to the system, as was done in [9, 4]. In the occultation inversion case, for instance, it is often assumed for regularization that the electronic density, $\rho(\vec{x})$, is a function of the radial coordinate only, i.e., that spherical symmetry holds locally. It should be clear from this discussion that what we have, in either case, is a linear inversion problem, and that although the mathematics involved in the analysis of each case may appear to be quite different, inverting delay data from orbiting (for GNSS reflections or occultation) or ground receivers is essentially the same type of problem.

5 Ionospheric combination: simulations

The *ionospheric combination* L_I , as seen in section 4 is designed to eliminate ranging differences due to geometry and other non-dispersive effects. Only ionospheric effects are left over. What happens in the GNSS-R case? An important question is whether it will be possible to track the GNSS-R signal phases of $E1$ and $E2$ (respectively, the electromagnetic field with carrier frequency $L1$ and $L2$) from space, or if the ionospheric combination can be somehow directly extracted (some possibilities have been identified). The ionospheric combination phase, obtained as the phase of the field $E1 \cdot E2^*$ should not be sensitive to the rugosity of the surface: it is characterized by an infinite synthetic wavelength. If we take the zeroth order approximation to the scattered field at a frequency f_i it will be of the form (h is the altitude)

$$F_i \approx \rho e^{iq_i h}. \quad (4)$$

Thus for the ionospheric combination

$$F_1 \cdot F_2^* \approx \rho^2, \quad (5)$$

i.e., within the validity of this approximation, there is no phase left. Our simulations confirm this behaviour: the ionospheric combination is not very sensitive to sea state, and its phase should be easily trackable. We discuss this now in more detail.

We first simulated 12 minutes of low altitude data from a static platform and 100 meters of altitude—the simulation corresponds to a code length of 11 meters, due

to the patch to altitude relationship. See figure 5 for some results. This is a simple situation, but it can already be compared to our other simulations with the usual L_{12} combinations. The difference is staggering, the ionospheric combination phase is not very sensitive to sea state. As usual, we expect a loss of correlation as the number of Fresnel zones is increased by a larger patch size. But it seems to indicate that the usual troubles of the GNSS-R signal are cured to some extent by the good properties of the ionospheric combination. In this sense, it seems again that the situation in GNSS-R is pretty reasonable for ionospheric phase studies.

According to recent spacecraft simulations [6] this behavior holds in space. The phase of the ionospheric combination behaves better than the phases of L_1 and L_2 considered separately. The phase of L_I shows less variability and noise.

These simulations (using is-GRADAS, [11]) considered a LEO scenario, with the receiving satellite at 500 km of height, moving at a speed of 7610 m/s. The sea surface is described as in [2]. The scattering process follows the specular points approach [5]. Basically, this approach is governed by three assumptions:

1. The backscattered power is dominated by specular reflections.
2. The power from each scatterer is characterised by its lifetime, radius of curvature, delay, Doppler and a random phase.
3. Under a Gaussian assumption, all necessary parameters can be deduced from an ocean surface elevation spectrum.

In figure 2 the phases of the fields of L_1 , L_2 , and L_I are shown, for a sea state characterised by a SWH of 0.3 m and a wind speed $U_{10} = 4$ m/s. Clearly the phase of the ionospheric combination is smoother than the other two phases. The same happens in figure 3, where the only change with respect to the previous figure is a higher wind speed and a higher SWH, respectively $U_{10} = 12$ m/s and $SWH = 2.9$ m. The two figures also point out the low sensitivity of the phase of L_I to sea surface conditions, considering that the two example can be considered as two opposite extreme sea state conditions.

Similar simulations has been carried out with another artificial GNSS-R signal generator called simply GRADAS (GNSS Reflections Artificial Data Synthesiser). This tool [11] has been developed starting from the consideration that it is not possible to simulate ocean surfaces over the total first chip zone in a LEO scenario. For example, considering a receiver at 500 km and the C/A code signal, the first chip zone represents, in a nadir-looking configuration, a disk of radius 17 km which, with a sampling of 20 cm, converts in a 85000×85000 matrix.

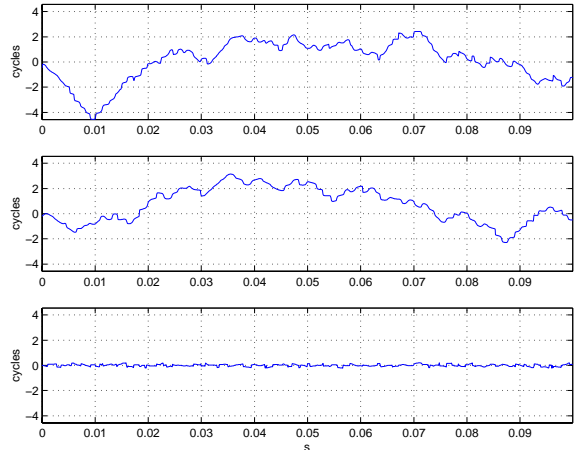


Figure 2: The three plots represent, from the top, the phase of the L_1 , L_2 , and L_I fields. The unit on the x-axis is seconds, on the y-axis cycles. The simulation assumes a LEO satellite at 500 km above the Earth, with a speed of 7610 m/s, a wind speed $U_{10} = 4$ m/s, and a significant wave height $SWH = 0.3$ m.

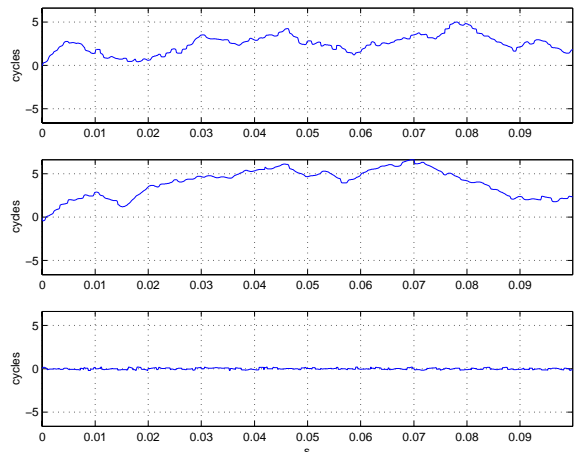


Figure 3: The three plots represent, from the top, the phase of the L_1 , L_2 , and L_I fields. The unit on the x-axis is seconds, on the y-axis cycles. This simulation, almost a worst case as far as the sea state condition is concerned, assumes again a LEO satellite at 500 km above the Earth, with a speed of 7610 m/s but a wind speed $U_{10} = 12$ m/s and a significant wave height $SWH = 2.9$ m.

To overcome this problem, as it has been suggested also in [10], that the scattered field can be computed only from a restricted sample of “small” patches, randomly distributed over the entire first chip zone.

6 Conclusions

Ionospheric delays can be estimated using GNSS-R due to dual or multiple frequency GNSS systems being available, or exploiting the difference in delay between code and phase (the one suffering a group velocity delay, the other a phase velocity delay) if only one frequency is available. We discussed above the potential accuracy from a high gain mission, e.g. with an antenna of 25 dB. In the context of low gain missions (with antenna gains of about 15 dB), such dual frequency code measurements would also be of great interest to the ionospheric research community. Using dual frequency code pseudo-ranges, current models predict that the ionospheric combination double-slant delays could be measured to better than a 2 meter after 1 second of integration, leading to vertical TEC measurements of about 15 TECU accuracy after 1 second, or about 3 TECU after 20 second averaging. Recall that for the GPS L_I combination (using L1 and L2) 1 TECU is equivalent to 10.5 cm of L_I delay and that typical TEC is between 0 and 50 TECU.

The expected accuracy of single frequency code-phase delay measurements would also be very useful (the error being dominated by the code part of the measurements).

The use of phase measurements would increase even more the interest of ionospheric GNSS-R measurements. We have seen indications in our simulations that the phase of the ionospheric combination is very well behaved after scattering, as expect from the use of an “infinite” synthetic wavelength (using the language in the PARIS Interferometric Processor context). This could imply that accurate GNSS-R ionospheric phase measurements will be possible from space. Moreover, the behaviour of ionospheric phase, according to our simulation, is not sensitive to sea state conditions.

It is known that ionospheric electron content data measured along vertical directions, when ingested in global ionospheric models, highly enhances the accuracy of such models since they complement occultation soundings. Little data with this characteristics is presently available over the oceans, and the vertical character of GNSS-R soundings together with their availability above water (and perhaps ice or land) covered areas (figure 4 [13]) will be able to fill these gaps.

ACKNOWLEDGEMENTS

We wish to thank the European Space Agency for its support through the PARIS-Beta project (ESTEC Con-

tract No. 15083/01/NL/MM) and other GNSS-R PARIS related projects (OPPSCAT, PIPAER, PARIS-Alpha, OPPSCAT 2).

REFERENCES

- [1] G. Born, A. Komjathy, P. Axelrad, and S. Crump-ton. Towards ingesting ionospheric data of surface reflected gps signals into global ionospheric models. In *Proceedings of the Ionospheric Determination and Specification for Ocean Altimetry and GPS Surface Reflection Workshop*, 1997.
- [2] T. Elfouhaily, B. Chapron, K. Katsaros, and D. Vandemark. A unified directional spectrum for long and short wind-driven waves. *Journal of Geophysical Research*, 1997.
- [3] M. Martin-Neira. A PASSive Reflectometry and Interferometry System (PARIS): application to ocean altimetry. *ESA Journal*, 17:331–355, 1993.
- [4] A. Rius, G. Ruffini, and L. Cucurull. Improving the vertical resolution of ionospheric tomography with GPS occultations. *Geophysical Research Letters*, 1997.
- [5] G. Ruffini, M. Caparrini, and B. Chapron. Improved ocean and em models for in-silico spaceborne gnss-r. Technical report, PARIS Beta WP3200 - ESA ESTEC CONTRACT No. 15083/01/NL/MM, 2001.
- [6] G. Ruffini, M. Caparrini, O. Germain, F. Soulat, and J. Lutsko. Remote sensing of the ocean by bistatic radar observations: a review. Technical report, PARIS Beta WP1000 - ESA ESTEC CONTRACT No. 15083/01/NL/MM, 2001.
- [7] G. Ruffini, E. Cardellach, A. Rius, and J.M. Aparicio. Remote sensing of the ocean by bistatic observations: a review. Technical report, WP1000 report for ESA contract 13461/99/NL/GD, 1999. Available online at <http://www.starlab-bcn.com>.
- [8] G. Ruffini, L. Cucurull, A. Flores, and A. Rius. A PIM-aided kalman filter for gps tomography of ionospheric electron content. *Physics and Chemistry of the Earth*, 1999.
- [9] G. Ruffini, A. Flores, and A. Rius. GPS tomography of the ionospheric electron content with a correlation functional. *IEEE Transactions on Geoscience and Remote Sensing*, 1999.
- [10] G. Ruffini, O. Germain, F. Soulat, M. Caparrini, J. Lutsko, and B. Chapron. Modelling of the received

signal characteristic. Technical report, PARIS Alpha WP2000 - ESA contract 14285/85/nl/pb, 2001.

- [11] G. Ruffini, F. Soulat, B. Chapron, M. Caparrini, O. Germain, and K. Sharman. GRADAS: a tool for GNSS-R scattering simulation. Technical report, PARIS Beta WP3100 - ESA ESTEC CONTRACT No. 15083/01/NL/MM, 2001.
- [12] E. Sardón, A. Rius, and N. Zarraoa. Estimation of the transmitter and receiver differential biases and the ionospheric total electron content from global positioning system observations. *Radio Science*, 29(3):577–586, 1994.
- [13] K. Sharman. Matlab code for orbit and specular point calculations. Technical report, STARLAB Barcelona SL, 2001.
- [14] P. Silvestrin. Earth-observation applications of navigation satellites. Technical report, Earth Observation Future Programmes Department, ESA Directorate of Application Programmes, ESTEC.

Data & User	MSS/W	H	DMSS	biTEC	biTROP
Weather Forecasting	Y				Y
Climate Research	Y	Y		Y	Y
Space Weather				Y	
Storm Detection	Y		Y		
Ship routing	Y		Y		
Fast boat routing	Y		Y		
Oil spill detection	Y				
Flood monitoring		Y			
River/lake level		Y			
Tide gauge		Y			
Tsunami detection		Y			
Oceanographic research		Y	Y		

Table 1: PARIS data products and their users.

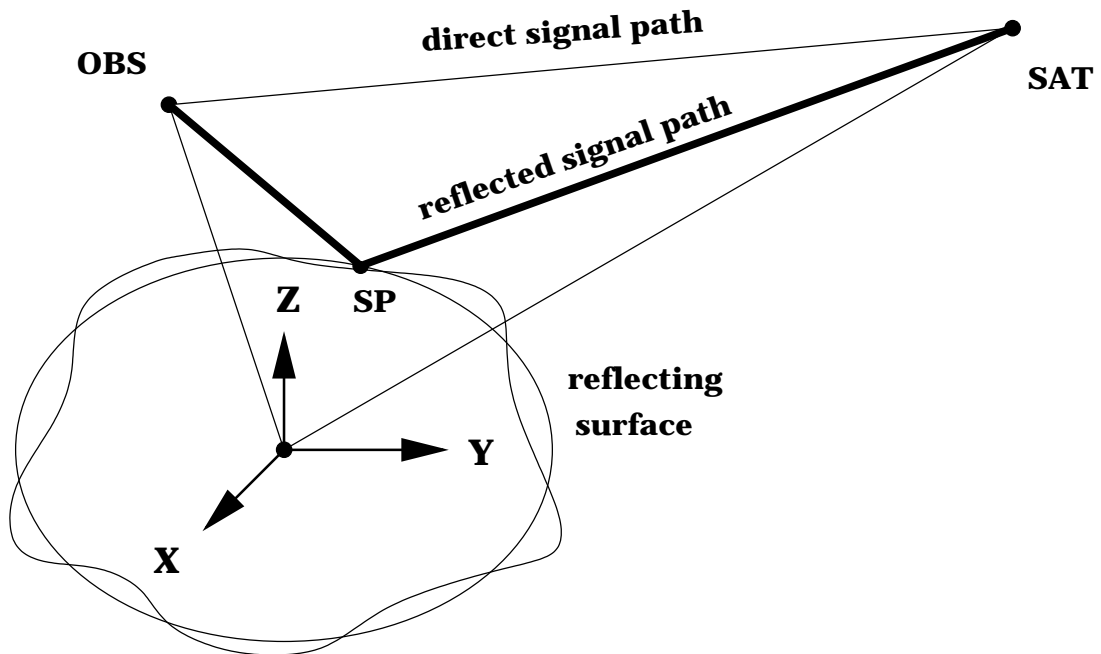


Figure 1: Schematic drawing of specular reflection over the geoid.

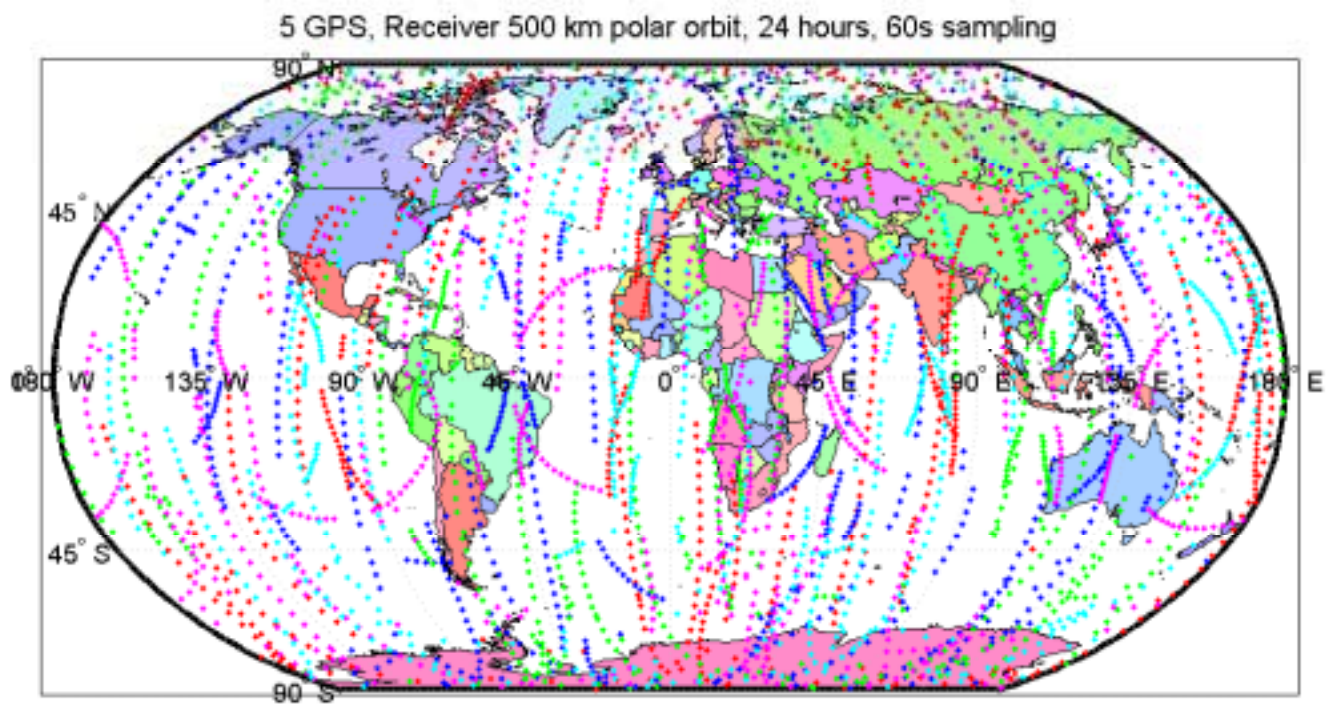


Figure 4: In this figure the specular points of reflection for a LEO satellite (polar orbit at 500 km), are shown. The time considered is one day. The simulation take into account only 5 satellites of the GPS constellation. The sampling time is one minute. We note that no cutoff has been used on the angle of incidence.

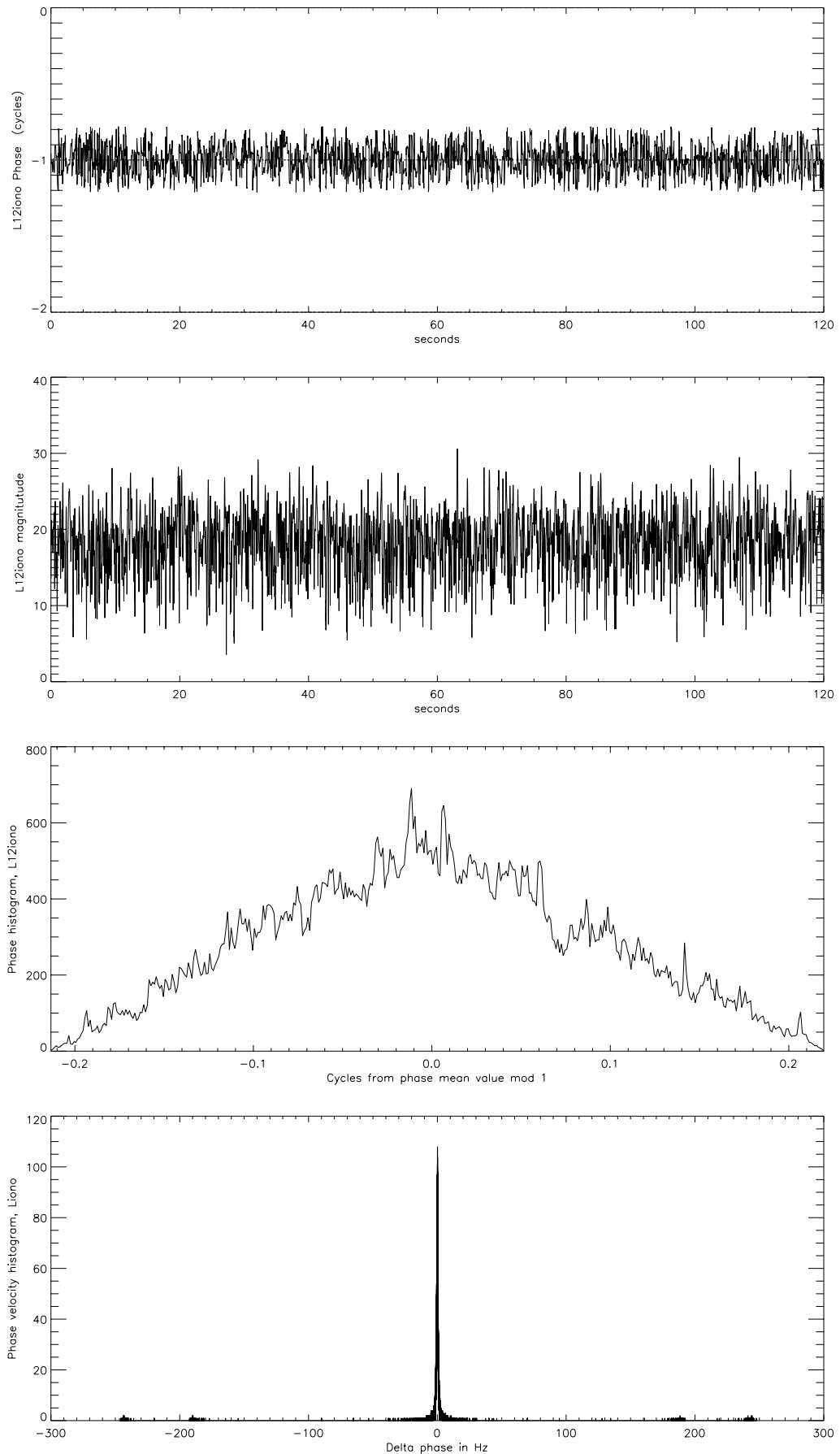


Figure 5: This is a histogram of the L_{12} ionospheric combination (at 0.001 cycles bin size) for a 12 minute simulation at 1 ms temporal resolution, $U_{10} = 8$ m/s, with a 256 times 0.2 cm patch size (51 m) at 100 m receiver height. Ocean parameters are about 80 cm peak to peak and a standard deviation of 11.6 cm. The last graph is a phase velocity histogram, at 1 Hz bin size.

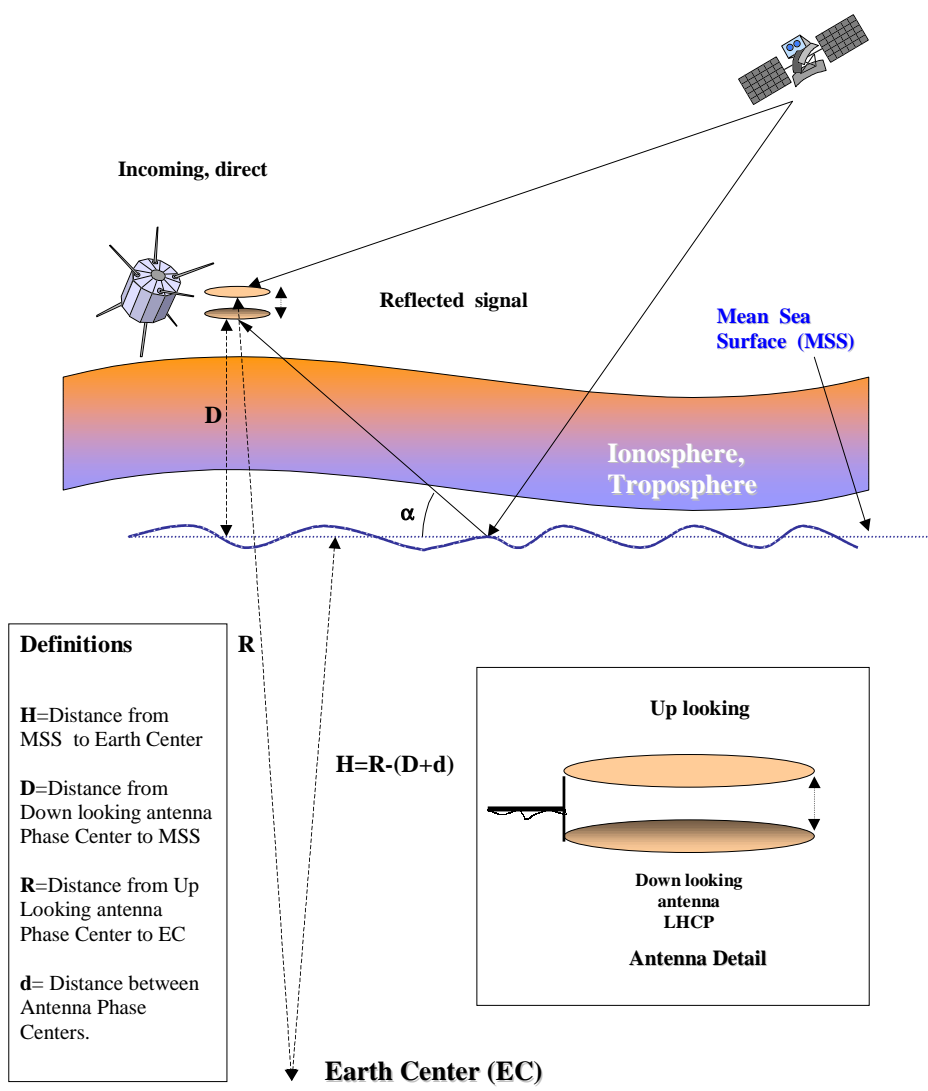


Figure 6: Schematic drawing of specular reflection ranging for spaceborne altimetry.